Project M
Stanford University
Stanford, California

Internal Memorandum
M Report No. M-289
December 1961

THE SINGLE-SCATTERING APPROXIMATION IN SKYSHINE PROBLEMS

By

K. G. Dedrick

I. INTRODUCTION

Skyshine problems are very complicated and are best handled using Monte Carlo methods with a high-speed computer. In some problems, the single-scattering approximation gives the dominant contribution to the scattered flux, and it always provides a limiting form for the more exact Monte Carlo calculations. These single-scattering calculations also provide a guide in the design of certain shields, and many shielding geometries can be immediately discarded on the basis of the single-scattering results.

The Poisson distribution provides a measure of the validity of the single-scattering approximation. Here we ask for the probability that n scattering events occur in a distance x when the mean free path is λ. This probability is

$$p_n = (1/n!)\ (x/\lambda)^n\ e^{-(x/\lambda)} \tag{1}$$

Figure 1* shows p_n as a function (x/λ) for the first few values of n. It is seen that single scattering gives the largest contribution to scattered flux for $0 \leq (x/\lambda) < 2$.

The geometry of the situation is shown in Fig. 2. A source of neutrons or other particles is at the point A. These are scattered through the angle θ at C to an observer at B. Integration over all points C then gives the total flux at B. In the method of integration used here, it is easy to include consideration of a shielding hill between A and B. This

*All figures are at the end of the text.

effect is included in the numerical results, which have been obtained under the assumption that nucleon-nucleon scattering is the most important process. The nucleon-nucleon cross section is considered to be isotropic in the center of mass, and is then transformed to the laboratory frame of reference. Other scattering cross sections can be introduced in the formulae presented.

II. FORMULAE FOR THE SCATTERED FLUX

The source of particles at A in Fig. 2 is described by an intensity $I(\alpha)$ which specifies the number of particles leaving A per second for unit solid angle about the angle α. The intensity of the beam scattered at C in the direction θ is then

$$e^{-(r_1/\lambda)} [I(\alpha) \ N_0 \ \sigma(\theta)/r_1^2] \ d\tau \tag{2}$$

where N_0 is the number of scattering centers per unit volume, $\sigma(\theta)$ is the differential scattering cross section, $d\tau$ is the differential volume element at C, and the factor $\exp(- r_1/\lambda)$ accounts for attenuation along the path where the mean free path is λ. At B, the flux due to scattering at C is $[\exp(- r_2/\lambda)]/r_2^2$ times the value given by (2), or

$$e^{-(r_1/\lambda)} \ e^{-(r_2/\lambda)} \ [I(\alpha) \ N_0 \ \sigma(\theta)/(r_1^2 \ r_2^2)] \ d\tau \tag{3}$$

The total flux ψ at B is then given by integrating over the volume V which includes all points C contributing to the flux, viz:

$$\psi = \int_V d\tau \ I(\alpha) \ N_0 \ \sigma(\theta) \ e^{-(r_1/\lambda)} \ e^{-(r_2/\lambda)}/(r_1^2 \ r_2^2) \tag{4}$$

This flux is clearly in units of particles per second per unit area at B.

The polar angles taken with AB as the polar axis are α and the azimuthal angle φ. These two angles and the angle θ of Fig. 2 will be used, rather than the usual polar coordinates (r_1,α,φ), in performing the integrations in Eq. (4). From Fig. 2, we have

$$x^2 = r_1^2 + r_2^2 + 2r_1 r_2 \cos\theta \tag{5a}$$

$$r_2 \sin\theta = x \sin\alpha \tag{5b}$$

Using these expressions, the volume element $d\tau$ may be calculated in terms of a Jacobian as follows:

$$d\tau = \frac{\partial(x_1,y_1,z_1)}{\partial(\theta,\alpha,\varphi)} \, d\theta \, d\alpha \, d\varphi \tag{6}$$

where (x_1,y_1,z_1) are the Cartesian coordinates of the point C. Rather than evaluate the determinant $\partial(x_1,y_1,z_1)/\partial(\theta,\alpha,\varphi)$, it is easier to make changes in the volume element for spherical polar coordinates,

$$d\tau = r_1^2 \sin\alpha \, dr_1 \, d\alpha \, d\varphi \tag{7}$$

by replacing dr_1 by $(\partial r_1/\partial\theta)_\alpha \, d\theta$. The derivative $(\partial r_1/\partial\theta)_\alpha$ is easily obtained from (5) and may be written $r_2^2/(x \sin\alpha)$. Using (7), the Jacobian in (6) is seen to be

$$\frac{\partial(x_1,y_1,z_1)}{\partial(\theta,\alpha,\varphi)} = \frac{r_1^2 \, r_2^2}{x} \tag{8}$$

so that (4) becomes

$$\psi = (1/x) \int d\theta \, d\alpha \, d\varphi \, e^{-(r_1/\lambda)} \, e^{-(r_2/\lambda)} \, I(\alpha) \, N_0 \, \sigma(\theta) \tag{9}$$

The angle φ is integrated over the range π, and the ranges of integration of the angles θ and α are determined by the shape of a shielding hill placed between the points A and B.

III. SHIELDING HILLS

We can easily calculate the effect on the scattered flux of a shielding hill having a triangular cross section such as shown in Fig. 3. The hill is to be a figure of revolution about the axis AB. The hill is assumed to be completely absorbing in this calculation, and its effect is found by placing the proper limits on the integrations over θ and α indicated in Eq. (9). If the actual hill under consideration is not of triangular cross section, or the point B is not chosen at an apex of the triangle as shown in Fig. 3, we can still compute the effect of the hill by circumscribing it by a triangle having an apex at B. This procedure is shown in Fig. 4 and gives us an equivalent triangular hill which changes as the point of observation B is varied.

At this point, a further approximation is made. The exponential factors in (9) complicate the integrations considerably. We can make a conservative approximation by removing them from (9) and multiplying the final result by $\exp(-x/\lambda)$. The flux calculated in this way will then be greater than the flux calculated using (9). On using this approximation, and considering the shielding hill, Eq. (9) becomes:

$$\psi \lesssim \frac{\pi N_o e^{-(x/\lambda)}}{x} \int_{\alpha_o}^{\pi} d\alpha \, I(\alpha) \int_{\alpha+\beta_o}^{\pi} \sigma(\theta) \, d\theta \tag{10a}$$

$$= \pi \, [1/(\Lambda x)] \, e^{-(x/\lambda)} \int_{\alpha_o+\beta_o}^{\pi+\beta_o} d\alpha' \, I(\alpha' - \beta_o) \, f(\alpha') \tag{10b}$$

where we define

$$f(\alpha') = \int_{\alpha'}^{\pi} \frac{\sigma(\theta)}{\sigma_o} \, d\theta \tag{11}$$

In obtaining (10b) from (10a), we have replaced $N_o\sigma_o$ by $1/\Lambda$, where Λ is the scattering mean free path, and σ_o is the total scattering cross section.

The procedure to be followed in these calculations is now clear. First choose $\sigma(\theta)$ and calculate $f(\alpha')$ using (11). The flux is then estimated by folding $f(\alpha')$ with $I(\alpha' - \beta_o)$ as in (10b).

IV. THE ISOTROPIC NUCLEON-NUCLEON CROSS SECTION IN THE CENTER OF MASS

As an example, we have calculated $f(\alpha')$ for the case where the source at A consists of neutrons which are scattered by nucleons in the nuclei of air molecules. It is then assumed that the nucleon-nucleon scattering cross section is isotropic in the center of mass of the two-nucleon systems. From the Lorentz transformation, we find that the scattering cross section in the laboratory frame of reference is

$$\sigma(\theta) = \begin{cases} \dfrac{(1 - \beta^2) \cos \theta}{\pi(1 - \beta^2 \cos^2 \theta)^2} \sigma_0 ; & 0 \leqslant \theta \leqslant \pi/2 \\ \\ 0 & ; \; \pi/2 \leqslant \theta \leqslant \pi \end{cases} \tag{12}$$

where σ_0 is the total scattering cross section, and β is $(1/c) \times$ (velocity of center of mass), i.e.,

$$\beta = [1 + (2M/E_k)]^{-\frac{1}{2}} \tag{13}$$

In (13), M is the nucleon rest energy, and E_k is the kinetic energy of the incident neutron.

For $\sigma(\theta)$ given by (12), the integral in Eq. (11) is elementary and yields

$$f(\alpha') = \frac{1}{2\pi} \left\{ 1 - \frac{\sin \alpha'}{(1 - \beta^2 \cos^2 \alpha')} + \frac{1}{\sqrt{\beta^2(1 - \beta^2)}} \left[\tan^{-1}\left(\frac{\beta}{\sqrt{1 - \beta^2}}\right) - \tan^{-1}\left(\frac{\beta \sin \alpha'}{\sqrt{1 - \beta^2}}\right) \right] \right\} \tag{14}$$

Values of $2\pi f(\alpha')$ are shown in Fig. 5 and tabulated in Table I for several values of the incident neutron energy E_k.

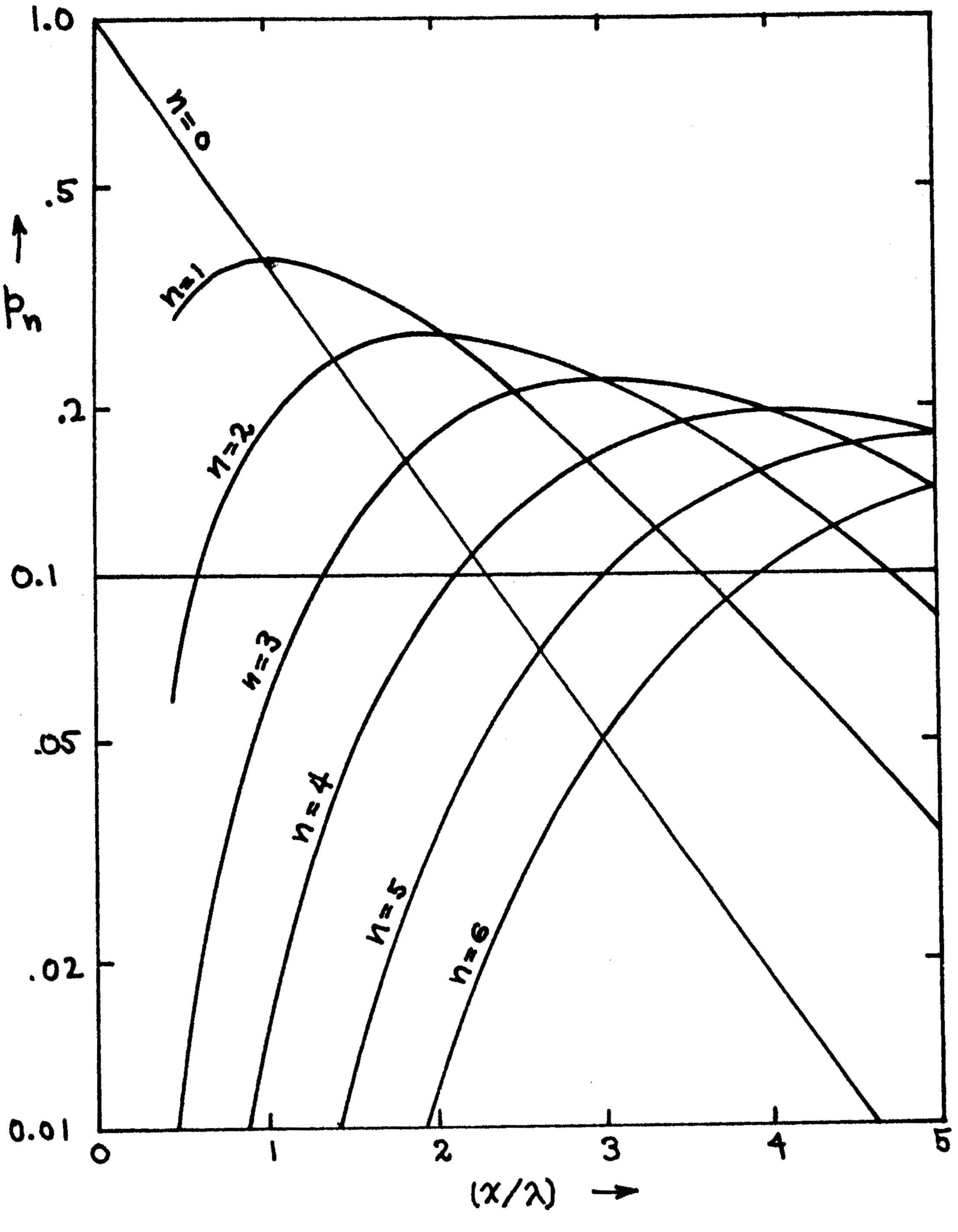

FIG. 1--Poisson distribution; probability of n events vs number of mean free paths.

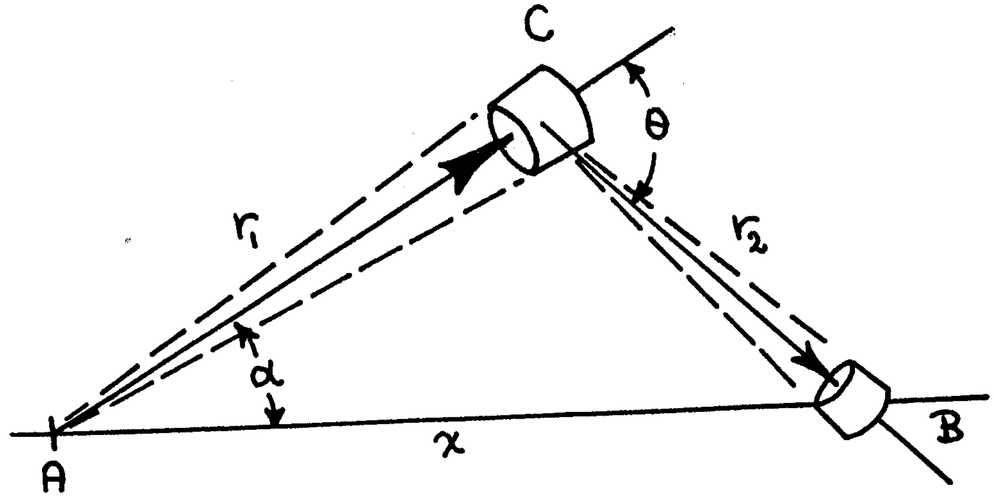

FIG. 2--Single scattering geometry.

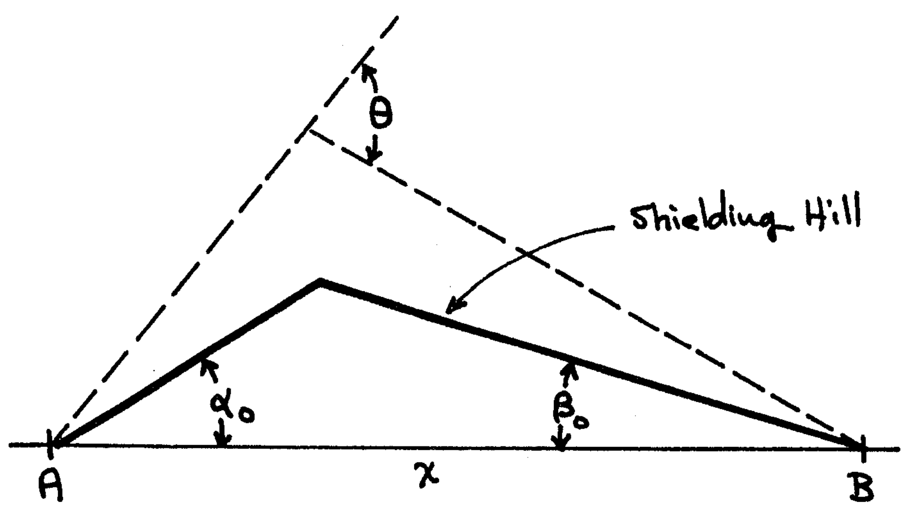

FIG. 3--The simple shielding hill.

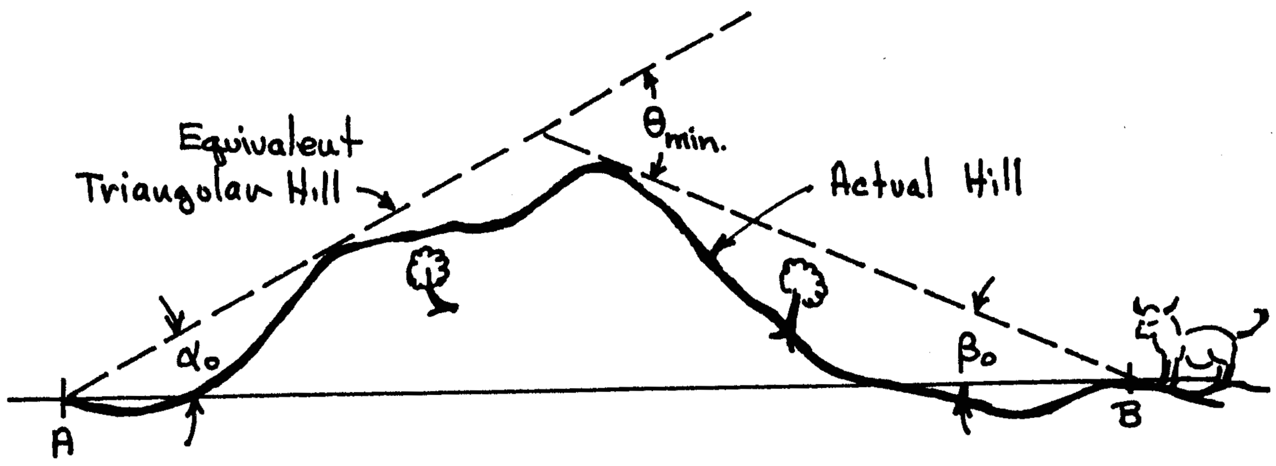

FIG. 4--The equivalent triangular hill.

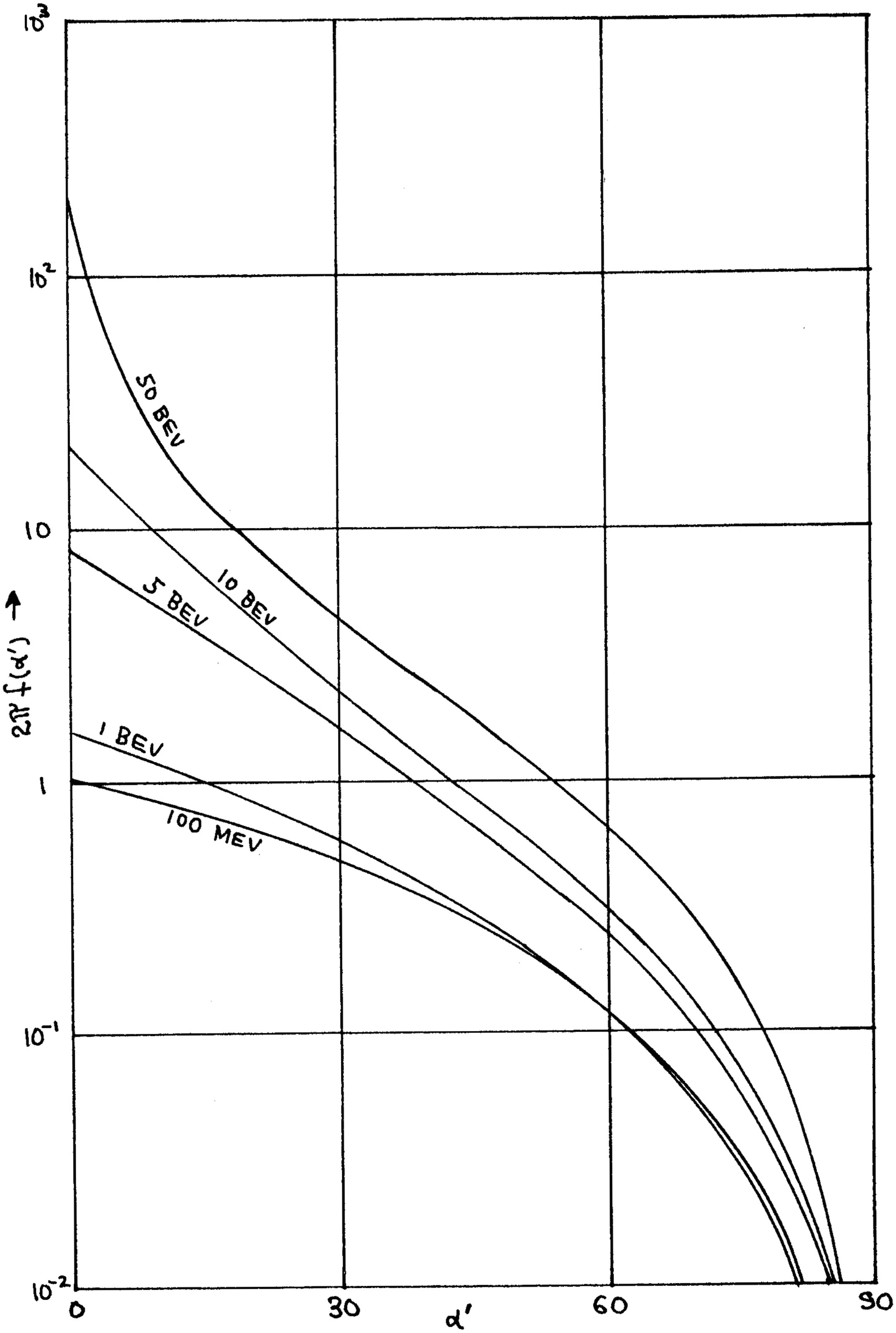

FIG. 5--Plot of Eq. (13) for several values of incident neutron energy E_k.

α'	Incident neutron energy E_k 100 Mev	500 Mev	1.0 Bev	5.0 Bev	10 Bev	50 Bev
0°	1.0129	1.1703	1.5479	8.2486	21.241	219.81
5°	0.9200	1.0449	1.3623	6.5694	14.328	51.653
10°	0.8282	0.9220	1.1825	5.0681	9.3874	23.366
15°	0.7379	0.8032	1.0115	3.8324	6.2500	13.626
20°	0.6505	0.6908	0.8529	2.8726	4.2872	8.9474
25°	0.5666	0.5861	0.7089	2.1469	3.0255	6.2607
30°	0.4847	0.4900	0.5806	1.6039	2.1783	4.5301
40°	0.3421	0.3260	0.3719	0.8922	1.1687	2.4859
50°	0.2207	0.1997	0.2207	0.4827	0.6261	1.3652
60°	0.1246	0.1079	0.1168	0.2404	0.3109	0.6840
70°	0.05548	0.04644	0.05009	0.0984	0.1273	0.2804
80°	0.01391	0.01138	0.01328	0.02346	0.03062	0.06833
90°	0.0	0.0	0.0	0.0	0.0	0.0

TABLE I--The function $2\pi\ f(\alpha')$ of Eq. (13) for various incident neutron energies.